Inorganic Chemistry

Article

pubs.acs.org/IC

Highly Selective Sorption of Small Hydrocarbons and Photocatalytic Properties of Three Metal–Organic Frameworks Based on Tris(4-(1*H*-imidazol-1-yl)phenyl)amine Ligand

Hong-Ru Fu,[†,‡] Yao Kang,[†] and Jian Zhang*[,†]

[†]State Key Laboratory of Structural Chemistry, Fujian Institute of Research on the Structure of Matter, Chinese Academy of Sciences, Fuzhou, Fujian, 35002, P. R. China

[‡]University of Chinese Academy of Science, 100049, Beijing, P. R. China

Supporting Information

ABSTRACT: By employing a tris(4-(1*H*-imidazol-1-yl)-phenyl)amine (Tipa) ligand, three new metal–organic frameworks, $[Zn_2(Tipa)(4,4'\text{-bpdc})_{1.5}(H_2O)(NO_3)]\cdot 2(DMF)\cdot H_2O$ (**1**; 4,4′-bpdc = 4,4′-biphenyldicarboxylate, DMF = *N*,*N*-dimenthylformamide), $[Cd(Tipa)Cl_2]\cdot 2(DMF)\cdot H_2O$ (**2**), and $[Co(Tipa)Cl_2(H_2O)]\cdot DMF\cdot H_2O$ (**3**), have been synthesized solvothermally. Compound **1** features a three-dimensional (3D) pillared-layer structure with low band gap and interesting photocatalytic properties. Compound **2** is a 2-fold interpenetrating (3,6)-connected porous framework, and it shows highly selective adsorption of C_2H_2, CO_2, and C_2H_4 over CH_4. Compound **3** with honeycomb-like layers exhibits unusual 2D + 2D→ 3D polycatenation (2D = two-dimensional). The luminescent properties for these compounds were also investigated.

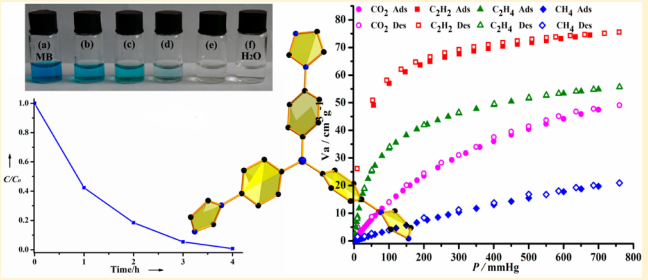

INTRODUCTION

Functional metal–organic frameworks (MOFs) are of great interest in recent years because of their aesthetic structures and potential applications on gas storage, separation, catalysis, and so on.[1] Practically, a variety of examples have demonstrated that the physical and chemical properties of the linkers play a decisive role in the structures and functions of novel MOFs.[2] Many rigid or flexible tripodal ligands, such as 2,4,6-tris(4-pyridyl)-1,3,5-triazine,[3] 2,4,6-tris[4-(1*H*-imidazole-1-yl)-phenyl]-1,3,5-triazine,[4] 1,3,5-tris(1-imidazolyl)benzene,[5] and $BH(mim)_3Na$ (mim = 2-methylimidazolate),[6] have been employed to synthesize new MOF structures with notable functions. Among them, the rigid ligands are in favor of constructing highly porous and robust frameworks for gas storage and separation, while the flexible ligands can adopt various conformations and make changeable frameworks.[7]

Recently, considering the high surface areas and good stability of some MOFs, they may be good photocatalytic materials for green degradation of organic dyes.[8] The advantages of MOFs as photocatalysts over other traditional metal oxide semiconductors lie in their special structural features, because the existence of inorganic and organic moieties leads to unusual metal–ligand charge transfer. It has been demonstrated that a triphenylamine group with good hole-transporting ability is expected to modify the electrical conductivity of the material effectively.[9] Triphenylamine can not only act as a strong electron donor in its initial state but can also stabilize the charge-transferred state. Meanwhile, the pore surface of MOF can be systematically functionalized by −OH, $-NH_2$, or −Cl groups to optimize its interaction with different gas molecules.[10] The adsorption and separation of small hydrocarbons by using MOFs are of great interest in recent years.[11] Here, a new tris(4-(1*H*-imidazol-1-yl)phenyl)amine (Tipa) ligand was synthesized from tris(4-bromophenyl)amine and imidazole by using the Ullmann condensation method. This Tipa ligand can have not only the cooperative organocatalytic center, but also the integration of flexible and long rigid characters. MOFs based on this Tipa ligand are rarely known to date.

In this work, three new MOFs, $[Zn_2(Tipa)(4,4'\text{-bpdc})_{1.5}(H_2O)(NO_3)]\cdot 2(DMF)\cdot H_2O$ (**1**; 4,4′-bpdc = 4,4′-biphenyldicarboxylate, DMF = *N*,*N*-dimenthylformamide), $[Cd(Tipa)Cl_2]\cdot 2(DMF)\cdot H_2O$ (**2**), and $[Co(Tipa)Cl_2(H_2O)]\cdot DMF\cdot H_2O$ (**3**), were synthesized under solvothermal conditions. Compound **1** displays the excellent photocatalytic degradation efficiency for organic dye. Remarkably, compound **2** shows highly selective adsorption of C_2H_2 and C_2H_4 over CH_4. Besides these findings, the luminescent properties for these compounds were also investigated.

EXPERIMENTAL SECTION

Materials and Instrumentation. All reagents were purchased commercially and used without further purification. The purity of all

Received: February 10, 2014
Published: April 4, 2014

   dx.doi.org/10.1021/ic5003226 | *Inorg. Chem.* 2014, 53, 4209–4214

Table 1. Crystal Data and Structure Refinements for Compounds 1−3

frameworks	1	2	3
formula	$C_{54}H_{45}O_{13}N_9Zn_2$	$C_{33}H_{35}O_3N_8Cl_2Cd$	$C_{30}H_{31}O_3N_7Cl_2Co$
formula weight	1157.63	774.25	667.34
crystal system	triclinic	orthorhombic	monoclinic
space group	$P\bar{1}$	*Pnna*	C_2
a (Å)	8.4804(3)	25.6632(5)	26.150(10)
b (Å)	14.1017(6)	15.0315(3)	15.464(5)
c (Å)	20.7617(9)	17.7572(3)	9.002(3)
α (deg)	83.472(4)	90.00	90.00
β (deg)	81.241(4)	90.00	103.994(6)
γ (deg)	82.823(3)	90.00	90.00
Z	2	8	4
V (Å^3)	2423.30(17)	6850.0(2)	3532(2)
μ (Mo/Cu Kα) (mm^{-1})	0.710 73	1.541 78	0.710 73
F(000)	976	1.541 78	1212
temperature (K)	293	293	293
θmin, max (deg)	2.4398, 29.1212	3.4047, 74.4189	2.3317, 27.6139
T_{min} and T_{max}	0.811, 0.811	0.342, 0.364	0.819, 0.876
R(int)	0.0512	0.0326	0.0298
N_{ref}, N_{par}	8545, 6266	7027, 5938	8148, 6091
R_1,wR $[I \geq 2\sigma(I)]^a$	0.0613, 0.1912	0.0543, 0.1489	0.0608, 0.1778
S	1.151	1.080	1.040
R_1, wR_2 (all data)	0.0820, 0.2061	0.0588, 0.1523	0.0674, 0.1835

$^a R_1 = \Sigma||F_o| - |F_c||/\Sigma|F_o|$. $wR_2 = \{\Sigma[w(F_o^2 - F_c^2)^2]/\Sigma[w(F_o^2)^2]\}^{1/2}$; where $w = 1/[\sigma^2(F_o^2) + (aP)^2 + bP]$ and $P = (F_o^2 + 2F_c^2)/3$.

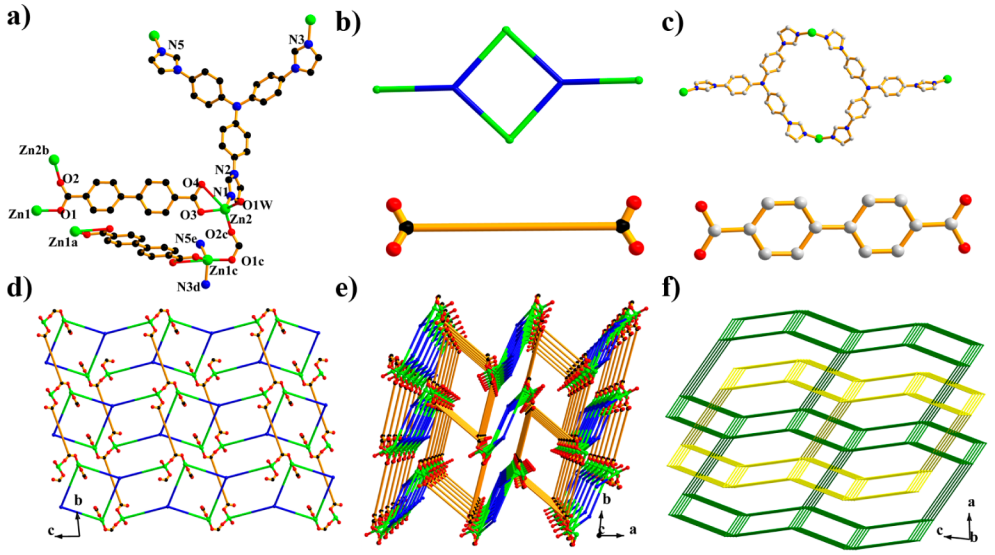

Figure 1. (a) The coordination environment in **1**; (b, c) the four-member ring and the 4,4′-bpdc linker; (d) the layer in **1**; (e) the 3D structure of **1**; (f) the 2-fold interpenetrating (3,6)-connected topology.

gases is 99.999%. The tris(4-(1*H*-imidazol-1-yl)phenyl)amine ligand was synthesized according to the reported procedures.[12] The powder X-ray diffraction (PXRD) analyses were carried out on a MiniFlex-II diffractometer with Cu Kα radiation (λ = 1.540 56 Å) with a step size of 1.0° (Supporting Information, Figures S1−3). Thermal stability studies were carried out on a NETSCHZ STA-449C thermoanalyzer with a heating rate of 10 °C/min under an air atmosphere (Supporting Information, Figures S4−6). Gas adsorption measurement was performed in the ASAP (Accelerated Surface Area and Porosimetry) 2020 System. Fluorescence spectra were measured with a HORIBA Jobin-Yvon FluoroMax-4 spectrometer.

Synthesis of [Zn_2(Tipa)(4,4′-bpdc)$_{1.5}$(H_2O)(NO_3)]·2(DMF)·H_2O (1). A mixture of Tipa (0.0225 g, 0.05 mmol), 4,4′-H_2bpdc (0.0225 g, 0.08 mmol), $Zn(NO_3)_2{\cdot}6H_2O$ (0.0560 g, 0.2 mmol), one drop of mineralization triethylamine, and DMF/MeOH/H_2O/DMSO (v:v:v:v 4:1:1:2, 8 mL) was heated in a 20 mL scintillation vial at 120 °C for 24 h and then cooled to room temperature. Colorless block crystals of **1** were obtained and dried in air (38.4 mg, 64% yield, based on Tipa ligand). Elemental analysis for $C_{54}H_{45}O_{13}N_9Zn_2$, Calcd. (%): C, 23.90; H, 1.66; N, 4.65. Found: C, 24.12; H, 1.64; N, 4.71.

Synthesis of [Cd(Tipa)Cl_2]·2(DMF)·H_2O (2). A mixture of Tipa (0.0225g, 0.05 mmol), L-proline (0.0115 g, 0.10 mmol), $CdCl_2{\cdot}4H_2O$ (0.0340 g, 0.2 mmol), and DMF/H_2O (v:v 2:0.5, 2.5 mL) was heated in a 20 mL scintillation vial at 100 °C for 24 h and then cooled to room temperature. Colorless block crystals of **2** were obtained and dried in air (29.2 mg, 73% yield, based on Tipa ligand). Elemental analysis for $C_{33}H_{35}O_3N_8Cl_2Cd$, Calcd. (%): C, 51.16; H, 4.52; N, 14.47. Found: C, 50.85; H, 4.63; N, 14.22.

Synthesis of [Co(Tipa)Cl_2(H_2O)]·DMF·H_2O (3). A mixture of Tipa (0.0225g, 0.05 mmol), L-proline (0.0115 g, 0.10 mmol), $CoCl_2{\cdot}$

dx.doi.org/10.1021/ic5003226 | *Inorg. Chem.* 2014, 53, 4209−4214

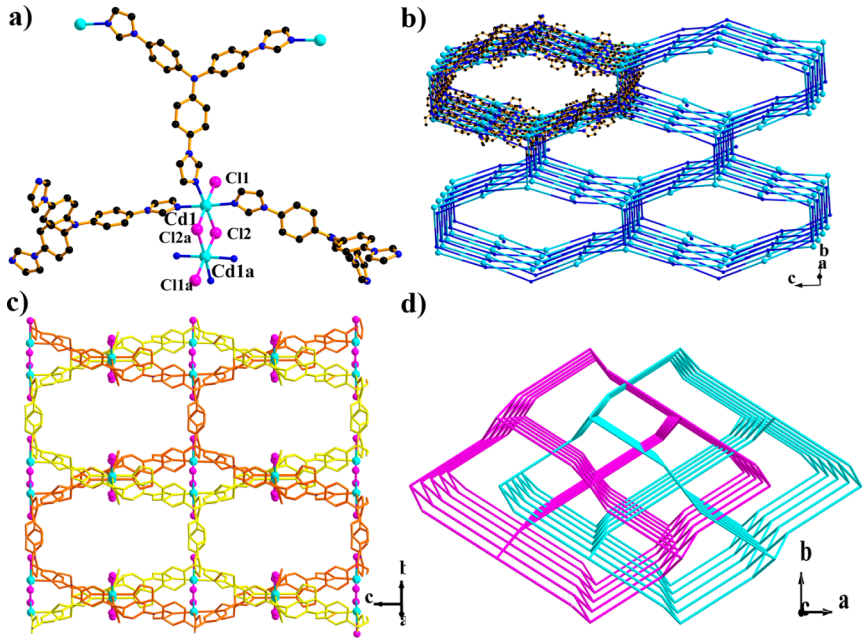

Figure 2. (a) Coordination environment of the Cd(II) ions in **2**; (b) the Cd-Tipa framework in **2**; (c) a simple framework containing two Cd-Tipa frameworks linked by the μ_2-Cl^- ions; (d) the 2-fold interpenetrating (3,6)-connected net of **2**.

$6H_2O$ (0.0340 g, 0.2 mmol), and DMF/H_2O (v:v 2:1, 3 mL) was heated in a 20 mL scintillation vial at 80 °C for 16 h and then cooled to room temperature. Claret-colored block crystals of **3** were obtained and dried in air (27.3 mg, 79% yield, based on Tipa ligand). Elemental analysis for $C_{30}H_{31}O_3N_7Cl_2Co$, Calcd. (%): C, 53.97; H, 4.65; N, 14.69. Found: C, 53.85; H, 4.71; N, 14.34.

X-ray Diffraction Analysis. Suitable single crystals of **1**−**3** were carefully selected under an optical microscope and glued to thin glass fibers, whereafter single-crystal X-ray diffraction analyses were performed on a computer-controlled XCalibur E CCD diffractometer with graphite monochromated Mo Kα radiation ($\lambda_{Mo\ K\alpha}$ = 0.710 73 Å) at T = 293 K. The structures were solved by using the direct method and refined by full-matrix least-squares methods on F^2 by using the SHELX-97 program package.[13] Non-hydrogen atoms were refined anisotropically. The SQUEEZE option of PLATON[14] was used to eliminate the contribution of disordered guest molecules to the reflection intensities. Crystallographic data for compounds **1**−**3** were listed in Table 1.

RESULTS AND DISCUSSION

Description of Crystal Structures. *[Zn_2(Tipa)(4,4′-bpdc)$_{1.5}$(H_2O)(NO_3)]·2(DMF)·H_2O (**1**).* In the structure of compound **1**, the Zn1 atom is coordinated by three oxygen atoms from two 4,4′-bpdc ligands and two nitrogen atoms from two different Tipa ligands (Figure 1a), making the Zn1 atom a 4-connecting node. The Zn2 atom is coordinated by three oxygen atoms from two 4,4′-bpdc ligands, one water molecule, and one Tipa nitrogen atom. Each Tipa ligand links three Zn atoms. As shown in Figure 1c, two zinc ions are bridged by two tipa ligands to form a four-member ring, and then these four-member rings are connected by the 4,4′-bpdc ligands into a layer (Figure 1d). Furthermore, the resulting layers are joined into a three-dimensional (3D) framework with the 4,4′-bpdc ligands as the pillars (Figure 1e). The resulting architechure is a 2-fold interpenetrating framework. From the viewpoint of topology, each dinuclear zinc unit and the Tipa ligand can be regarded as 6- and 3-connected nodes, respectively. Thus the framework of **1** can be simplified as a (3,6)-connected net with vertex symbol of $(4.4.6_3)$ $(4.4.4.4.6.6.6_3.6_3.6_3.6_3.6_4.6_4.8_{12})$ (Figure 1f).

*[Cd(Tipa)Cl_2]·2(DMF)·H_2O (**2**).* In the structure of compound **2**, the Cd atom with distorted octahedral geometry is coordinated by three N atoms from three different Tipa ligands, two μ_2-Cl^- ions, and a terminal Cl^- ion (Figure 2a). Each Tipa ligand links three Cd atoms, acting as a 3-connected node. The Cd−Cl and Cd−N lengths are in the normal range.[15] Without the bridge of all μ_2-Cl^- ions, the Cd(II) ions are linked by the Tipa ligands into a 3-connected 3D framework with large open channels (Figure 2b). Two resulting frameworks are further joined together by the μ_2-Cl^- ions, forming an interlacing architecture with large rectangular channels (Figure 2c). Because of the large voids in a simple framework, a final 2-fold interpenetrating structure of **2** is generated. According to a calculation using PLATON program, the interpenetrated framework still contains a solvent-accessible void space of 33.0% of the total crystal volume. In the structure of **2**, the dinuclear Cd_2Cl_2 unit can be regarded as a 6-connected node, and the Tipa ligand is considered as a 3-connected node. Thus the whole structure of **2** can be simplified as a (3,6)-connected net (Figure 2d).

*[Co(Tipa)Cl_2(H_2O)]·DMF·H_2O (**3**).* In the structure of **3**, each Co atom has a slightly distorted octahedral coordination environment with three imidazole N atoms from three different tipa ligands, one O atom from the coordinated water molecule, and two terminal Cl ions in the opposite direction (Figure 3a). Each Tipa ligand acts as a tridentate ligand and connects three Co centers. The Co centers are linked by the Tipa ligands to form a honeycomb-like (6,3) layer (Figure 3b). As shown in Figure 3c, inclined interpenetration was observed between the layers. There are two sets of layers oriented toward different directions. These two sets of layers catenate to each other in a parallel−parallel arrangement to form a 2D + 2D → 3D (2D = two-dimensional) inclined polycatenation structure (Figure 3d). The dihedral angle of two interpenetrated 2D layers is 55.66 Å. There is no direct covalent interaction between

dx.doi.org/10.1021/ic5003226 | Inorg. Chem. 2014, 53, 4209−4214

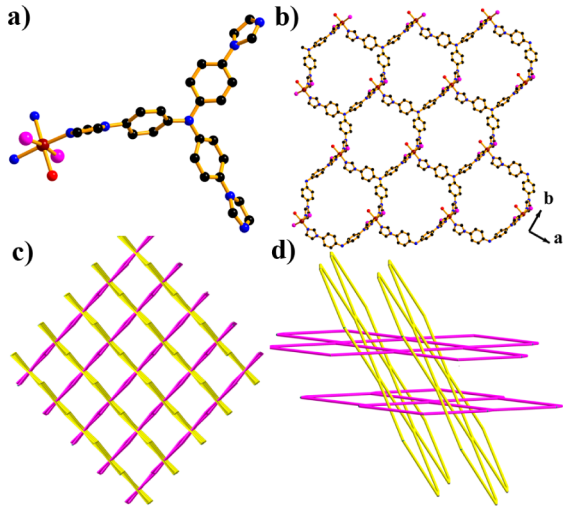

Figure 3. (a) Coordination environment in **3**; (b) the honeycomb-like layer in **3**; (c) the inclined polycatenation structure of **3**; (d) the interpenetrating details in the structure of **3**.

interpenetrated layers, and structural stability is kept by weak intermolecular interactions.

Photocatalytic Properties of 1. The band gap of compound **1** was measured by a solid state ultraviolet−visible (UV−vis) diffuse reflection measurement method at room temperature. According to the equation $\alpha h\nu^2 = K(h\nu - E_g)^{1/2}$ (where $h\nu$ is the discrete photo energy, α is the absorption coefficient, E_g is the band gap energy, and K is a constant), the extrapolated values (the straight lines to the x axis) of $h\nu$ at α = 0 give absorption edge energy corresponding to E_g = 2.55 eV for compound **1**. To study the photocatalytic activity of compound **1**, we select methylene blue (MB) as a model of dye contaminant to evaluate the photocatalytic effectiveness. The experiments were performed in typical processes. A suspension containing **1** (40 mg) and 80 mL of MB (4.0×10^{-5} mol L^{-1}) solution was stirred in the dark for about 30 min. Then, the mixture was stirred continuously under UV irradiation from a 350 W xenon lamp. A sample solution (2 ml) was taken every 30 min or 1 h and separated through centrifuge to remove suspended catalyst particles, while the starting point did not contain the first 30 min to rule out the effect of its absorption on the material surfaces. After filtration, the samples were analyzed by the UV−vis spectrophotometry. By contrast, the simple photolysis experiment was also completed under the same conditions without any catalyst. The organic dye concentrations were estimated by the absorbance at 665 nm (MB). Interestingly, approximately 58% of MB was decomposed during the first hour. After 4 h, the MB in the solution almost disappeared (Figure 4). The results indicate that compound **1** has a high photocatalytic activity for the degradation of MB. Additionaly, the powders were obtained by filtration after photocatalytic reaction, and the PXRD patterns of each powder were basically identical to those of the parent compounds, indicating that these complexes are stable during photocatalysis (Supporting Information, Figure S1).

Luminescent Properties. The photoluminescent properties of compounds **1** and **2** were investigated in the solid state at room temperature. The emission peaks of the compounds are shown in Figure 5. Compound **1** exhibits an intense emission between 430 and 575 nm (λ_{max} = 487 nm upon excitation at 349 nm). The maximum emission peaks at about

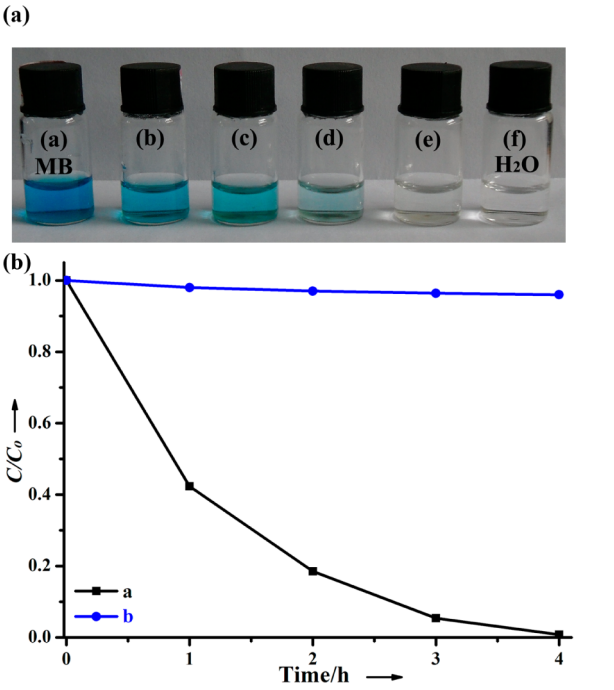

Figure 4. (a) Photograph of photocatalytic degradation of MB on **1**; (b) photocatalytic decomposition of MB solution with the changes in C/C_0 plot of compound **1** (black line), and the control experiment without any catalyst (blue line).

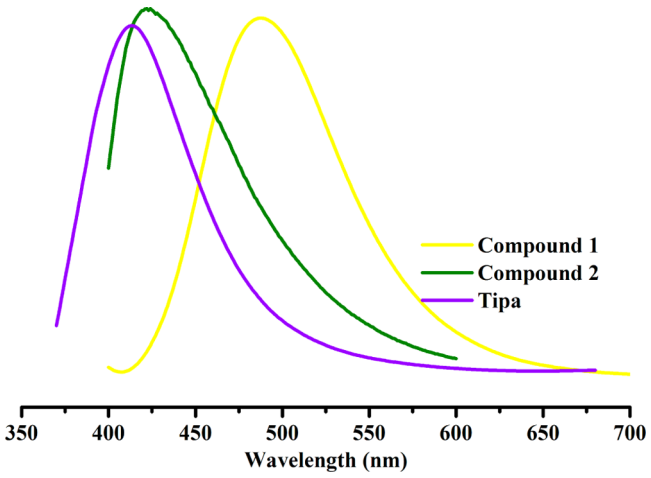

Figure 5. The emission spectra of compounds **1**, **2**, and free Tipa ligand in the solid state at room temperature.

421 nm (λ_{ex} = 338 nm) were observed for compound **2**. The λ_{max} of free Tipa is 405 nm, while free 4,4′-bpdc ligand fluoresce in the solid state with their emission peaks at 396 nm.[16] However, we did not observe obvious peak in the range of 350−450 nm for **1**, indicating that there are no $\pi^*-\pi$ transitions between Tipa ligands and the deprotonated acids. So the emission peaks for **1** and **2** can be attributed to the charge transfer ($\pi\rightarrow\pi^*$ and $n\rightarrow\pi^*$) of internal Tipa ligands, and the red-shifted emission of **1** is attributed to the metal-to-ligand charge transfer (MLCT) transitions.

Gas Sorption Properties of Compound 2. To investigate the permanent porosity of compound **2**, gas sorption experiments evaluating N_2, H_2, and CO_2 uptakes were performed. The freshly prepared samples of compound **2** were first activated through solvent exchange with acetone 10

dx.doi.org/10.1021/ic5003226 | Inorg. Chem. 2014, 53, 4209−4214

times in 3 d, followed by the thermal/vacuum activation at 303 K to generate activated materials. As shown in Figure 6a, the N_2 sorption isotherm at 77 K shows that **2** displays typical Type I sorption behavior, with Langmuir and BET surface areas of 484.8 and 348.8 $m^2\ g^{-1}$, respectively. Meanwhile, it has a moderate absorption of H_2 (95.7 $cm^3\ g^{-1}$ STP, 0.89 wt %) at 77 K and 1 atm. The CO_2 uptakes around 1 atm are 48.17 and 33.49 $cm^3\ g^{-1}$ at 273 and 297 K, respectively (Figure 6b,c).

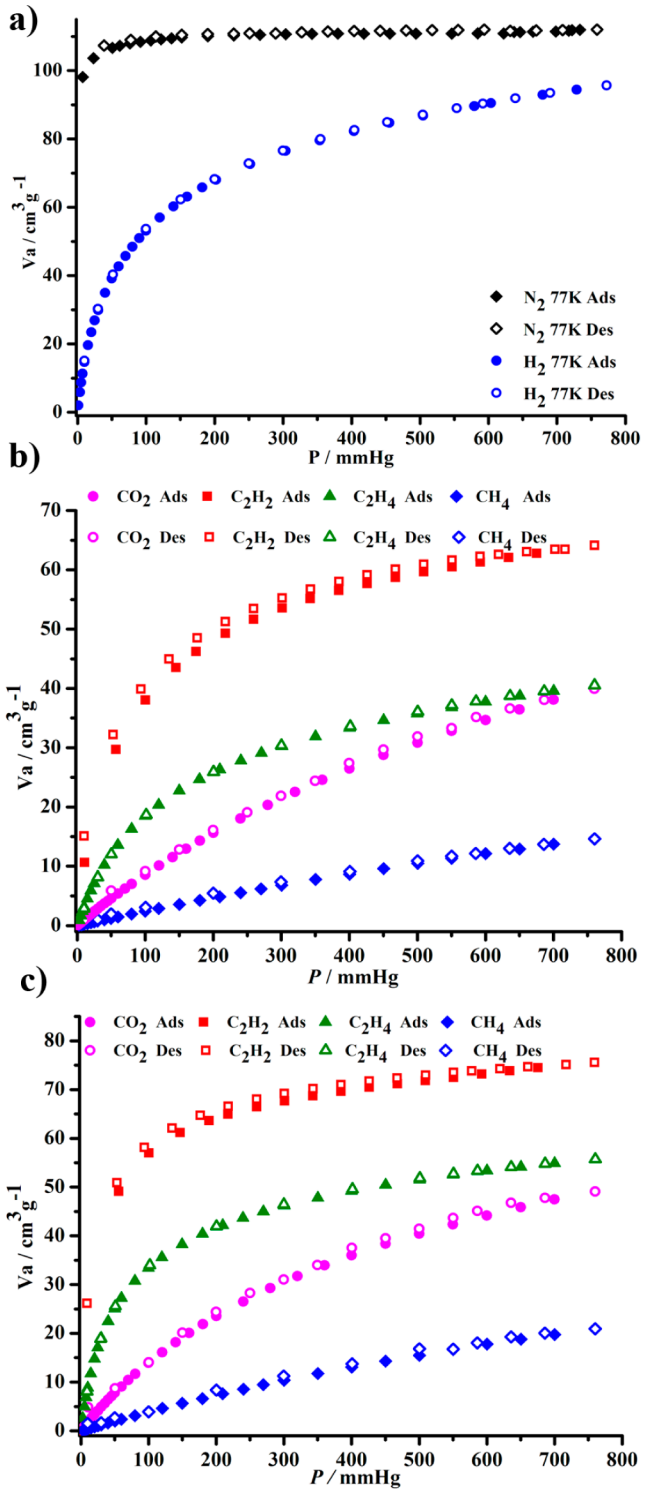

Figure 6. The gas sorption isotherms of **2**: (a) H_2 and N_2 sorption isotherms at 77 K; (b) C_2H_2, C_2H_4, CH_4, and CO_2 sorption isotherms at 297 K; (c) C_2H_2, C_2H_4, CH_4, and CO_2 sorption isotherms at 273 K.

The small hydrocarbons, CH_4, C_2H_2, and C_2H_4, are also selected as probe molecules to assess the gas adsorption properties of compound **2** (Figure 6b,c). As expected, compound **2** adsorbs much more C_2 hydrocarbons than C_1 methane. At 297 K and 1 atm, compound **2** can take up a moderate amount of C_2H_2 (64.13 $cm^3\ g^{-1}$) and C_2H_4 (40.52 $cm^3\ g^{-1}$), but basically a much smaller amount of CH_4 (12.04 $cm^3\ g^{-1}$), indicating that compound **2** is a promising material for selective separation of C_2 hydrocarbons from CH_4 at room temperature. To evaluate the affinity of gas molecules to compound **2**, we calculated the isosteric enthalpies of adsorption (Q_{st}) of CH_4, C_2H_2, and C_2H_6 from the adsorption data using the virial method at zero coverage. The Q_{st} value of CH_4 for **2** is 22.72 kJ/mol, while the Q_{st} values of C_2H_2 and C_2H_4 for **2** are 41.05 and 34.69 kJ/mol, respectively. It is worthy to mention that these Q_{st} values of C_2H_2 and C_2H_4 are much higher than those observed with other MOFs, such as M′MOF-4a[17] (36.0, 28.0 kJ/mol), M′MOF-2a[18] (30.0, 22.5 kJ/mol), and Zn-MOF-74[19] (32, 23 kJ/mol). These results indicate that the surface of **2** has strong affinity with the light hydrocarbons.

To evaluate the gas separation ability of **2**, the adsorption selectivities of C_2H_2/CH_4, C_2H_4/CH_4, and CO_2/CH_4 were calculated by Henry's law based on the equation $S_{ij} = KH(i)/KH(CH_4)$. The calculated selectivities for C_2H_2, C_2H_4, and CO_2 over CH_4 are 67.9, 23.7, and 4.3 at 273 K, 39.1, 13.5, and 3.1 at 297 K, respectively, which are higher and comparable to the previously reported porous adsorbents, such as UTSA-34b[20] (18−24), UTSA-35a[21] (15−25), and mesoPOF[22] (25−40). The C_2H_2/CH_4 selectivity in compound **2** is one of the few highest values ever reported among the porous metal−organic materials.[21,23] The highly selective sorption of **2** for C_2H_2 and CO_2 makes it a good candidate for practical C_2H_2/CH_4, C_2H_4/CH_4, and CO_2/CH_4 separation application in the near future.

CONCLUSIONS

In summary, three new MOFs based on the Tipa ligand were successfully synthesized. Compound **1** exhibits photocatalytic activity for the degradation of MB dye. Compound **2** is a promising microporous MOF for the selective adsorption of C_2H_2 and CO_2 over CH_4. Compound **3** shows interesting inclined polycatenation structure. The results reveal that these functional framework materials have potential applications in separation of gases and photocatalysis.

ASSOCIATED CONTENT

Supporting Information

Additional figures, TGA, powder X-ray diffraction patterns, luminescence photos, and CIF file. This material is available free of charge via the Internet at http://pubs.acs.org.

AUTHOR INFORMATION

Corresponding Author

*E-mail: zhj@fjirsm.ac.cn.

Notes

The authors declare no competing financial interest.

dx.doi.org/10.1021/ic5003226 | Inorg. Chem. 2014, 53, 4209−4214

■ ACKNOWLEDGMENTS

We thank the support of this work by 973 Program (2012CB821705 and 2011CB932504), NSFC (91222105, 21221001, 21173224), and CAS (XDA07070200).

■ REFERENCES

(1) (a) Yaghi, O. M.; O'Keeffe, M.; Ockwig, N. W.; Chae, H. K.; Eddaoudi, M.; Kim, J. *Nature* **2003**, *423*, 705−714. (b) Kitagawa, S.; Kitaura, R.; Noro, S. *Angew Chem., Int. Ed.* **2004**, *43*, 2334−2375. (c) Li, J. R.; Zhou, H. C. *Nat. Chem.* **2010**, *2*, 893−898. (d) Li, J. R.; Kuppler, R. J.; Zhou, H. C. *Chem. Soc. Rev.* **2009**, *38*, 1477−1504. (e) Herm, Z. R.; Wiers, B. M.; Mason, J. A.; van Baten, J. M.; Hudson, M. R.; Zajdel, P.; Brown, C. M.; Masciocchi, N.; Krishna, R.; Long, J. R. *Science* **2013**, *340*, 960−964. (f) Liu, Y.; Boey, F.; Lao, L. L.; Zhang, H.; Liu, X.; Zhang, Q. *Chem.—Asian J.* **2011**, *6*, 1004−1006. (g) Pullen, S.; Fei, H. H.; Orthaber, A.; Cohen, S. M.; Ott, Sascha. *J. Am. Chem. Soc.* **2013**, *135*, 16997−17003.

(2) (a) Zhang, M. W.; Chen, Y. P.; Bosch, M.; Gentle, T.; Wang, K. C.; Feng, D. W.; U. Wang, Z. Y.; Zhou, H. C. *Angew. Chem., Int. Ed.* **2014**, *53*, 815−818. (b) Xiong, W. W.; Athresh, E. U.; Ng, Y. T.; Ding, J. F.; Wu, T.; Zhang, Q. C. *J. Am. Chem. Soc.* **2013**, *135*, 1256−1259. (c) Feng, D. W.; Chung, W. C.; Wei, Z. W.; Gu, Z. Y.; Jiang, H. L.; Chen, Y. P.; Darensbourg, D. J.; Zhou, H. C. *J. Am. Chem. Soc.* **2013**, *135*, 17105−17110. (d) Gao, J. K.; He, M.; Lee, Z. Y.; Cao, W. F.; Xiong, W. W.; Li, Y. X.; Ganguly, R.; Wu, T.; Zhang, Q. C. *Dalton Trans.* **2013**, *42*, 11367−11370. (e) Zhao, X.; Bu, X. H.; Wu, T.; Zheng, S. T.; Wang, L.; Feng, P. Y. *Nat. Commun.* **2013**, *4*, 2344 DOI: 10.1038/ncomms3344. (f) Bu, F.; Lin, Q. P.; Zhai, Q. G.; Wang, L.; Wu, T.; Zheng, S. T.; Bu, X. H.; Feng, P. Y. *Angew. Chem., Int. Ed.* **2012**, *51*, 8538−8541.

(3) (a) Abrahams, B. F.; Batten, S. R.; Hamit, H.; Hoskins, B. F.; Robson, R. *Angew. Chem., Int. Ed.* **1996**, *35*, 1690−1692. (b) Lu, Z. Z.; Zhang, R.; Pan, Z. R.; Li, Y. Z.; Guo, Z. J.; Zheng, H. G. *Chem.—Eur. J.* **2012**, *18*, 2812−2824.

(4) Zheng, S. R.; Yang, Q. Y.; Liu, Y. R.; Zhang, J. Y.; Tong, Y. X.; Zhao, C. Y.; Su, C. Y. *Chem. Commun.* **2008**, *47*, 356−358.

(5) (a) Su, Z.; Fan, J.; Okamura, T. A.; Chen, M. S.; Chen, S. S.; Sun, W. Y.; Ueyama, N. *Cryst. Growth Des.* **2010**, *10*, 1911−1922. (b) Fan, J.; Gan, L.; Kawaguchi, H.; Sun, W. Y.; Yu, K. B.; Tang, W. X. *Chem.—Eur. J.* **2003**, *9*, 3965−3973.

(6) Zhang, H. X.; Wang, F.; Yang, H.; Tan, Y. X.; Zhang, J.; Bu, X. *J. Am. Chem. Soc.* **2011**, *133*, 11884−11887.

(7) (a) Zhao, D.; Timmons, D. J.; Yuan, D. Q.; Zhou, H. C. *Acc. Chem. Res.* **2011**, *44*, 123−133. (b) Farha, O. K.; Hupp, J. T. *Acc. Chem. Res.* **2010**, *43*, 1166−1175. (c) Paz, F. A. A.; Klinowski, J.; Vilela, S. M. F.; Tome, J. P. C.; Cavaleiro, J. A. S.; Rocha, J. *Chem. Soc. Rev.* **2012**, *41*, 1088−1110.

(8) (a) Yang, H.; He, X. W.; Wang, F.; Kang, Y.; Zhang, J. *J. Mater. Chem.* **2012**, *22*, 21849−21851. (b) Wen, L. L.; Zhou, L.; Zhang, B. G.; Meng, X. G.; Qua, H.; Li, D. F. *J. Mater. Chem.* **2012**, *22*, 22603−22609.

(9) (a) Rathore, R.; Burns, C. L.; Guzei, I. A. *J. Org. Chem.* **2004**, *69*, 1524−1530. (b) Shang, Y. L.; Wen, Y. Q.; Li, S. L.; Du, S. X.; He, X. B.; Cai, L. L.; Yang, L. M.; Gao, H. J.; Song, Y. L. *J. Am. Chem. Soc.* **2007**, *129*, 11674−11675.

(10) (a) Deshpande, R. K.; Minnaar, J. L.; Telfer, S. G. *Angew. Chem., Int. Ed.* **2010**, *49*, 4598−4602. (b) Kim, M.; Boissonnault, J. A.; Dau, P. V.; Cohen, S. M. *Angew. Chem., Int. Ed.* **2011**, *50*, 12193−12196. (c) Dau, P. V.; Tanabe, K. K.; Cohen, S. M. *Chem. Commun.* **2012**, *48*, 9370−9372. (d) Burtch, N. C.; Jasuja, H.; Dubbeldam, D.; Walton, K. S. *J. Am. Chem. Soc.* **2013**, *135*, 7172−7180.

(11) (a) Geier, S. J.; Mason, J. A.; Bloch, E. D.; Queen, W. L.; Hudson, M. R.; Brown, C. M.; Long, J. R. *Chem. Sci.* **2013**, *4*, 2054−2061. (b) Nijem, N.; Wu, H. H.; Canepa, P.; Marti, A.; Balkus, K. J.; Thonhauser, J. T.; Li, J.; Chabal, Y. J. *J. Am. Chem. Soc.* **2012**, *134*, 15201−15204. (c) He, Y.; Krishna, R.; Chen, B. L. *Energy Environ. Sci.* **2012**, *5*, 9107−9120.

(12) Wu, H.; Liu, H. Y.; Liu, Y. Y.; Yang, J.; Liu, B.; Ma, J. F. *Chem. Commun.* **2011**, *47*, 1818−1820.

(13) (a) Sheldrick, G. M. *Acta Crystallogr.* **2008**, *A64*, 112−122. (b) Sheldrick, G. M. *SHELXL-97,* Program for Crystal Structure Solution and Refinement; University of Göttingen: Göttingen, Germany, 1997.

(14) Spek, L. *PLATON;* The University of Utrecht: Utrecht, The Netherlands, 1999.

(15) (a) Wu, H.; Liu, H. Y.; Liu, B.; Yang, J.; Liu, Y. Y.; Ma, J. F.; Liu, Y. Y.; Ba, H. Y. *CrystEngComm* **2011**, *13*, 3402−3407. (b) Shipman, M. A.; Price, C.; Gibson, A. E.; Elsegood, M. R. J.; Clegg, W.; Houlton, A. *Chem.—Eur.J.* **2000**, *6*, 4371−4378. (c) Mishra, R.; Ahmad, M.; Tripathi, M. R. *Polyhedron* **2013**, *50*, 22−30. (d) Zhao, W.; Zhu, H. F.; Okamura, T.; Sun, W. Y.; Ueyama, N. *Supramol. Chem.* **2003**, *15*, 345−352.

(16) (a) Dai, J. C.; Wu, X. T.; Fu, Z. Y.; Cui, C. P.; Hu, S. M.; Du, W. X.; Wu, L. M.; Zhang, H. H.; Sun, R. Q. *Inorg. Chem.* **2002**, *41*, 1391−1396. (b) Huang, X. Y.; Yue, K. F.; Jin, J. C.; Liu, J. Q.; Wang, C. J.; Wang, Y. Y.; Shi, Q. Z. *Inorg. Chem. Commun.* **2011**, *14*, 952−955. (c) Guo, F.; Wang, F.; Yang, H.; Zhang, X. L.; Zhang, J. *Inorg. Chem.* **2012**, *51*, 9677−9682.

(17) Das, M. C.; Guo, Q. S.; He, Y. B.; Kim, J.; Zhao, C. G.; Hong, K. L.; Xiang, S. C.; Zhang, Z. J.; Thomas, K. M.; Krishna, R.; Chen, B. L. *J. Am. Chem. Soc.* **2012**, *134*, 8703−8710.

(18) Xiang, S. C.; Zhang, Z. J.; Zhao, C. G.; Hong, K.; Zhao, X. B.; Ding, D. R.; Xie, M. H.; Wu, C. D.; Das1, M. C.; Gill, R.; Thomas, K. M.; Chen, B. L. *Nat. Comm.* **2011**, *2*, 204−209.

(19) Bloch, E. D.; Queen, W. L.; Krishna, R.; Zadrozny, J. M.; Brown, C. M.; Long, J. R. *Science* **2012**, *335*, 1606−1610.

(20) He, Y.; Zhang, Z.; Xiang, S.; Wu, H.; Fronczek, F. R.; Zhou, W.; Krishna, R.; O'Keeffe, M.; Chen, B. L. *Chem.—Eur. J.* **2012**, *18*, 1901−1904.

(21) He, Y.; Zhang, Z.; Xiang, S.; Fronczek, F. R.; Krishna, R.; Chen, B. L. *Chem. Commun.* **2012**, *48*, 6493−6495.

(22) Katsoulidis, A. P.; Kanatzidis, M. G. *Chem. Mater.* **2012**, *24*, 471−479.

(23) Xu, H.; He, Y. B.; Zhang, Z. J.; Xiang, S. C.; Cai, J. F.; Cui, Y. J.; Yang, Y.; Qian, G. D.; Chen, B. L. *J. Mater. Chem. A* **2013**, *1*, 77−81.